J Mater Sci (2017) 52:12717–12723

Composites

Preparation of superparamagnetic and flexible γ-Fe_2O_3 nanowire arrays in an anodic aluminum oxide template

Xinxin Zhu[1], Jiangxia Fan[1], Yan Zhang[1], Hao Zhu[1], Bo Dai[1], Minhao Yan[1], and Yong Ren[1,*]

[1] *Department of Materials Science and Engineering, State Key Laboratory Cultivation Base for Nonmetal Composites and Functional Materials, Southwest University of Science and Technology, Mianyang, China*

Received: 10 May 2017
Accepted: 10 July 2017
Published online: 13 July 2017

ABSTRACT

Superparamagnetic and flexible Fe_2O_3 nanowire arrays were fabricated by the controlled electrostatic assembly of iron oxide nanoparticles and poly(dimethyldiallylammonium chloride) (PDADMAC) in an anodic aluminum oxide (AAO) template. The micrograph of iron oxide nanowire arrays was characterized by field emission scanning electron microscopy. The magnetic hysteresis loops obtained by a vibrating sample magnetometer confirm that the nanowire arrays have superparamagnetic properties. The filling ratio of iron oxide nanoparticles and polymers in the AAO template was affected by four factors, including the concentration of iron oxide nanoparticles, the pore diameter of the AAO template, the charge ratio of iron oxide nanoparticles and PDADMAC, and the molecular weight of polyacrylic acid. The effect of the AAO template on the diameter and length of the nanowire arrays was also analyzed. In addition, the nanowire arrays were shown to be flexible because of the presence of polymers. These nanowire arrays with superparamagnetic and flexural properties have potential applications in sensor probes.

Introduction

Magnetic nanowires have recently received considerable attention as a result of their potential applications, including photonics [1], electronics [2–4], sensing [5, 6], and biomedicine [7, 8]. Compared with traditional materials, nanomaterials have many novel properties, such as optical [9], electrical [10], thermal, and magnetic [11] properties. Nanowires, such as iron oxide, have received significant attention as useful candidates for biosensors because of their biocompatibility and magnetic properties. In a biosensor, a probe with nanobrush statically captures the biological signals. If we can control the movement of the nanobrush, the contact rate between the probe and the determined signals can be theoretically simultaneously improved, thereby greatly improving the sensitivity of the biosensor. We assumed that superparamagnetic and flexible nanowire arrays can sway with changes in the magnetic field, thus controlling the movement of the probe, meaning that the sensor sensitivity with these nanowire arrays can be improved.

Many methods have been used to fabricate iron oxide nanowires, including hydrothermal methods

Address correspondence to E-mail: reny2005@163.com

DOI 10.1007/s10853-017-1383-0

[12–14], electrospinning [15], and sol–gel methods [16]. The length and diameter of the iron oxide nanowires prepared by these methods are hard to control. Yan [17, 18] used an electrostatic self-assembly method for the preparation of superparamagnetic iron oxide nanowires. The nanowires had diameters of around 200 nm and lengths between 1 μm and 0.5 mm, with either positive or negative charges on their surface. However, the nanowires prepared by this way were dispersed in water and it was difficult to control the length and diameter of the nanowires. On the basis of their work, we first used the method combined with electrostatic self-assembly and an AAO template to prepare ordered nanowire arrays with superparamagnetic properties, as well as tunable diameter and length.

We report a novel and effective approach for the formation of iron oxide nanowire arrays. Because of the electrostatic interaction, negatively charged iron oxide nanoparticles and positively charged polymers can be assembled into nanowires using an AAO template under a stable magnetic field. The length and diameter of the nanowire arrays were controlled by the diameter and depth of the AAO template throughout the process.

Materials and methods

Materials

Poly(dimethyldiallylammonium chloride) (PDADMAC, $M_w < 100{,}000$) and polyacrylic acid (PAA, $M_w = 1800$ and $M_w = 800$) were procured from Sigma-Aldrich, Singapore. Aluminum (99.999% purity, 0.5 mm thickness) was procured from Beijing Technology Co., Ltd., China. AAO templates with a 400 nm pore diameter and a 30 μm thickness were procured from Shanghai Shangmu Technology Co. Ltd., China.

Fabrication

We prepared solutions to fabricate iron oxide nanowire arrays in the AAO template. Solution (I) was prepared by the mixture of a certain mass fraction of nanoparticle solution and a 1 mol L^{-1} NH_4Cl solution. Solution (II) was prepared by the mixture of PDADMAC and a 1 mol L^{-1} NH_4Cl solution. The PH values of these solutions mentioned above were adjusted to 7–8 by 10 wt% ammonia solution. Solution (III) was a mixture of solutions (I) and (II) under a certain charge ratio (Z). The relative amount of each component was monitored by the Z in solution (III). Z was defined as the ratio between the cationic charges borne by the polymers and the anionic charges carried by the particles at their surfaces. Then, the AAO template was immersed in solution (III) for a period of time, with the purpose of making the nanoparticles and polymer adequately filled with the AAO template. After, the sample was placed in ultra-pure water to dialysis with 0.5 T of the magnetic field for a period of time. In the whole process of dialysis, the ordered nanowire arrays were fabricated from the controlled electrostatic co-assembly of oppositely charged nanoparticles and commercially available polyelectrolytes, with the decrease in the concentration of NH_4Cl in the holes of the AAO template.

Characterization

Morphological analysis was performed with field emission scanning electron microscopy (FESEM, Ultra 55, Carl Zeiss Ltd., Jena, Germany). The magnetic hysteresis loops were obtained by a vibrating sample magnetometer (VSM, BKT-4500Z, Albert days of Beijing Science and Technology Co., Ltd.).

Results and discussion

Figure 1a, d shows typical FESEM images of the AAO template prepared by a two-step anodization process with a constant direct voltage of 45 V for 5 h in $C_2H_2O_4$ at 5 °C with a pore diameter of around 90 nm. Figure 1b, e shows typical FESEM images of the AAO template prepared by a hard anodization with a constant direct voltage of 120 V for 1 h in $C_2H_2O_4$ at 5 °C with a pore diameter of around 190 nm. Figure 1c, f shows typical FESEM images of the commercially available AAO template with a pore diameter of around 400 nm. The iron oxide nanoparticles investigated here were synthesized according to the Massart technique [17–19] by alkaline coprecipitation of iron (II) and iron (III) salts, oxidation of the magnetite (Fe_3O_4) into maghemite (γ-Fe_2O_3) nanoparticles and by size sorting of subsequent phase separations [20]. To improve their

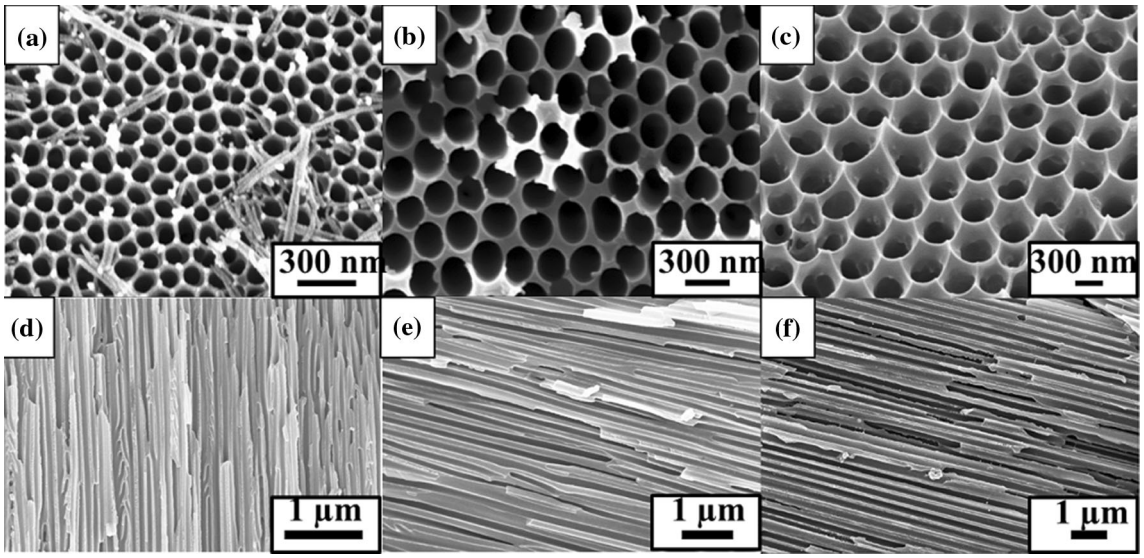

Figure 1 SEM of AAO template with different diameters; **a** and **d** were formed by traditional two-step anodization. **b** and **e** were formed by improved HA process. **c** and **f** were purchased AAO template.

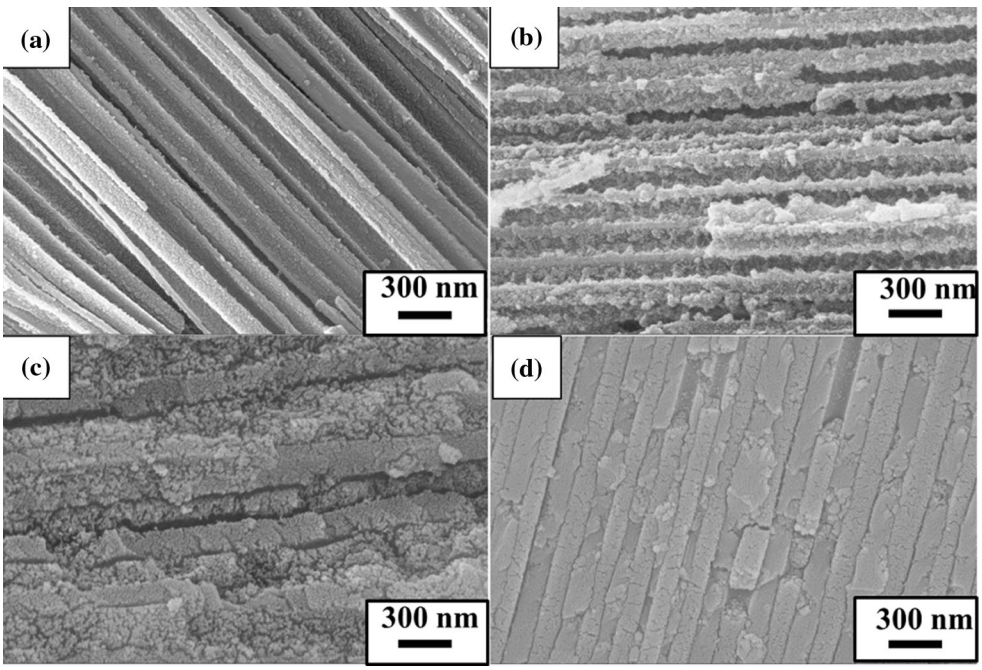

Figure 2 SEM of nanowires assembled with different concentration nanoparticles and PDADMAC under a 0.7 charge ratio in a pore diameter of 190 nm of AAO templates: **a** 1 wt%, $Z = 0.7$. **b** 2 wt%, $Z = 0.7$. **c** 3 wt%, $Z = 0.7$. **d** 4 wt%, $Z = 0.7$.

stability, the nanoparticles were coated with PAA using the precipitation dispersion technique [21].

It has been well established that several factors affect the filling ratio of iron oxide nanoparticles and polymers in the AAO template. First, the concentration of iron oxide particles affected the filling ratio. The AAO templates with a pore diameter of around 190 nm were immersed in a series of solutions with different concentrations of nanoparticles at $Z = 0.7$. Figure 2 shows the effect of different concentrations of iron oxide nanoparticles on the filling rate. Under the condition that the concentration of nanoparticles was less than 4 wt%, nanoparticles and cationic polyelectrolytes were attached to the pore walls of

the AAO template instead of assembling into nanowires. We decided that the reason why the nanoparticles and cationic polyelectrolyte polymers were easily attached to the hollow wall at lower concentrations of nanoparticles is because of the large specific surface energy of the pore wall of the AAO template. Thus, nanoparticles and PDADMAC were well filled into the pores of the AAO template and obtained a high filling ratio when the concentration of nanoparticles reached 4 wt%.

The pore diameters of the AAO templates are found to have a strong influence on the filling ratio in Fig. 3. At the pores of the AAO template around 90 nm, the nanoparticles and PDADMAC entered the pores of AAO template but barely assembled into nanowires. The result revealed that the pore

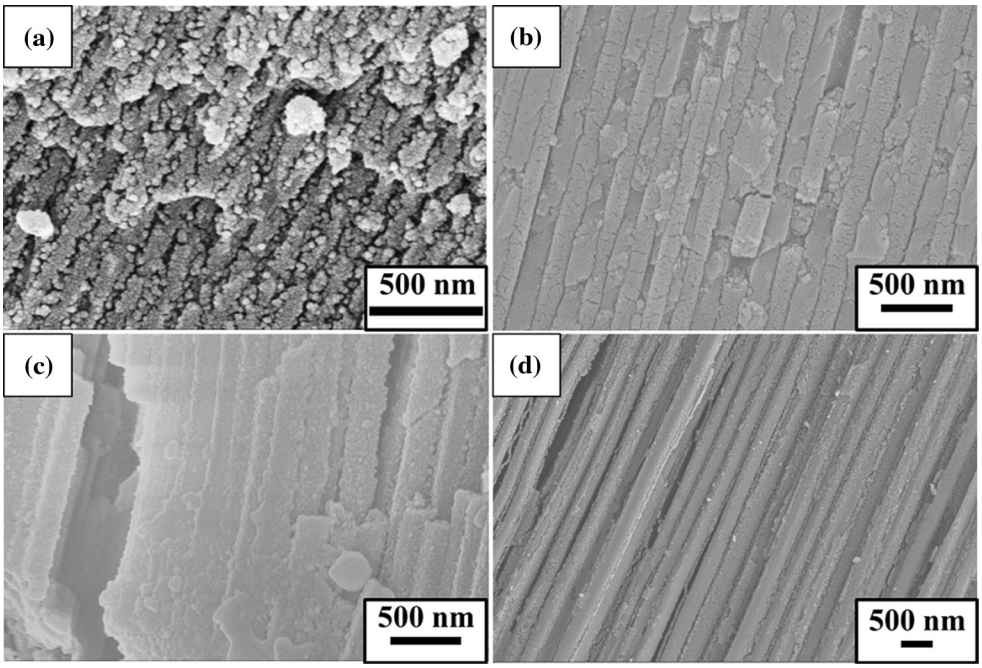

Figure 3 SEM of nanowires assembled in different diameters of AAO template: **a** 4 wt%, $Z = 0.7$, $D_p = 90$ nm. **b** 4 wt%, $Z = 0.7$, $D_p = 190$ nm. **c** 4 wt%, $Z = 0.7$, $D_p = 190$ nm. **d** 4 wt%, $Z = 0.7$, $D_p = 400$ nm.

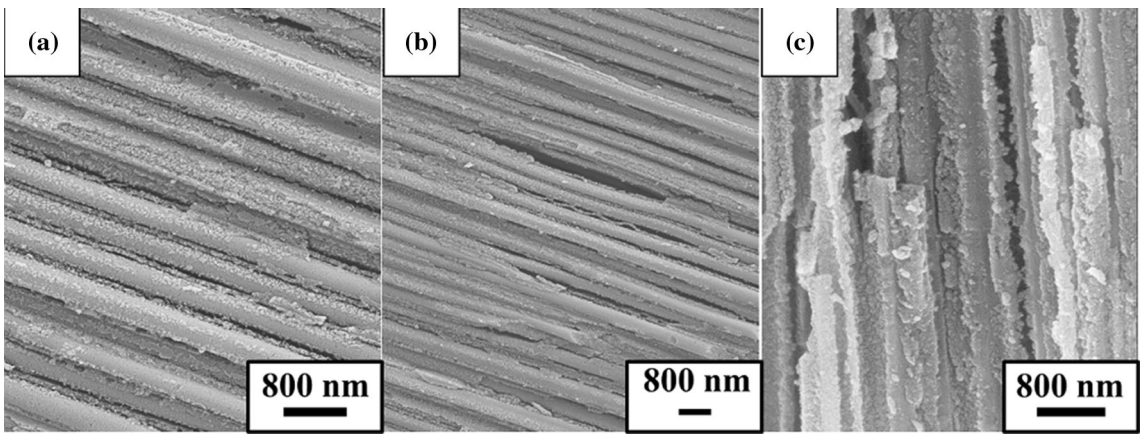

Fig. 4 SEM of nanowires assembled under different charge ratio Z: **a** 4 wt%, $Z = 0.35$, $D_p = 400$ nm. **b** 4 wt%, $Z = 0.7$, $D_p = 400$ nm. **c** 4 wt%, $Z = 7$, $D_p = 400$ nm.

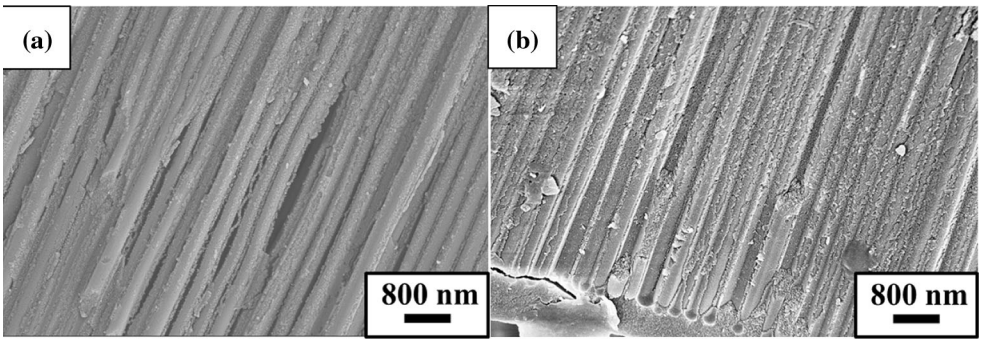

Fig. 5 SEM of nanowires assembled in diameter 400 nm of AAO templates with nanoparticles coated by different molecular weight PAA. **a** $M_W = 1800$ g mol^{-1}, **b** $M_W = 800$ g mol^{-1}.

diameters of the template are smaller, and the pore spaces between nanoparticles are larger. Figure 3b, c shows the middle and nozzle of the pores of the AAO template with a pore diameter of around 190 nm, respectively. Although γ-Fe_2O_3 nanoparticles and PDADMAC were better filled into the AAO templates, the assembled nanowires were loose and broken, as shown in Fig. 3b. At the nozzle of the AAO template, nanoparticles and PDADMAC were grown into dense nanowires. These results demonstrate that inadequate dialysis at the nozzle of the templates can easily form nanowires while the middle of AAO templates cannot. Iron oxide nanoparticles and PDADMAC were sufficiently assembled into nanowires in the AAO template form Fig. 3d.

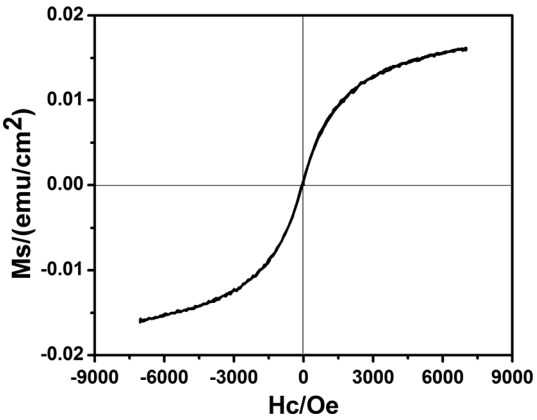

Fig. 6 Magnetic hysteresis loops of nanowire arrays.

The effect of the Z on the filling ratio is shown in Fig. 4. We found that the nanoparticles and the cationic polyelectrolyte polymer easily entered the pores of the AAO template and grew into nanowires at $Z = 0.35$ and 0.7. However, nanoparticles and the polymer were not grown into nanowires at $Z = 7$. Because of the action of static between anionic charges nanoparticles and the hole wall of the AAO template, nanoparticles could not easily enter into the hole of the AAO templates. The cationic polyelectrolyte polymers were easily attached to the hole wall of the AAO template, but a low concentration of cationic polyelectrolyte polymer ($Z = 7$) led to nanoparticles barely entering into the hole of the AAO template. The effect of PAA with different

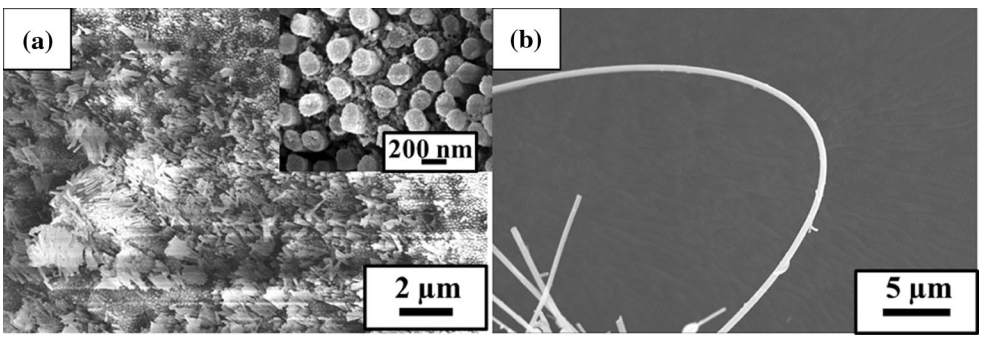

Fig. 7 **a** SEM of partial dissolution of the AAO template in 0.3 mol L^{-1} phosphoric acid for 20 min. **b** Morphology of nanowires after removal of AAO template.

molecular weights on the filling ratio was not significant (Fig. 5).

The magnetic hysteresis loops (Fig. 6) obtained by the VSM show that the nanowires have superparamagnetic properties. The result shows that iron oxide nanowires retained the superparamagnetic properties of iron oxide nanoparticles. By dissolution of the samples, we can obtain a nanobrush in the AAO template. Figure 7a shows the SEM of the nanowires prepared in the AAO template with a pore diameter of around 190 nm, and the thicker pore wall was corroded by 0.3 mol L^{-1} phosphoric acid for 20 min. It can be seen from the diagram that we obtained a nanobrush in AAO template. Figure 7b shows the morphology of nanowires after completely etching the AAO template in 0.3 mol L^{-1} phosphoric acid. We found that the nanowires were more flexible than fragile. It is likely that the improved flexibility is because of the presence of polymers.

Conclusions

A novel method combined with electrostatic assembly and the AAO template was used to fabricate superparamagnetic nanowires with controllable diameter and length. When the concentration of the nanoparticles was higher, the pore size of the AAO template was larger and the Z was smaller, and nanoparticles and cationic polyelectrolyte polymers were most easily assembled in the AAO template. Simultaneously, the molecular weight of PAA wrapped on the surface of the nanoparticles had no effect on the result of the assembly process. Using 0.3 mol L^{-1} phosphoric acid, we can obtain completely ordered nanowire arrays. The hysteresis loops of nanowires were measured using VSM, where the coercivity and remanence are almost zero, to perform a typical superparamagnetism. Therefore, superparamagnetic and flexible γ-Fe_2O_3 nanowire arrays have potential applications for improving sensor sensitivity.

Acknowledgments

This work was supported by the Program for Young Science and Technology Innovation Team of Sichuan Province (No. 2017TD0020), NSF of China (Grant Nos. 11304256 and 11505163), and the Project of State Key Laboratory Cultivation Base for Nonmetal Composites and Functional Materials (Nos. 14tdfk07 and 15zxfk10).

Compliance with ethical standards

Conflict of interest The authors declare that they have no conflict of interest.

References

[1] Toufiq AM, Wang F, Javed QUA, Li Q, Li Y (2014) Hydrothermal synthesis of MnO_2, nanowires: structural characterizations, optical and magnetic properties. Appl Phys A 116:1127–1132

[2] Lee CH, Kim DR, Zheng Z (2011) Fabrication of nanowire electronics on nonconventional substrates by water-assisted transfer printing method. Nano Lett 11:3435–3439

[3] Hong S, Lee H, Lee J, Kwon J, Han S, Suh YD, Cho H, Shin J, Yeo J, Ko SH (2015) Highly stretchable and transparent metal nanowire heater for wearable electronics applications. Adv Mater 27:4744–4751

[4] Hong I, Angelucci M, Verrelli R, Betti MG, Panero S, Croce F, Mariani C, Scrosatie B, Hassoun J (2014) Electrochemical characteristics of iron oxide nanowires during lithium-promoted conversion reaction. J Power Sources 256:133–136

[5] Liu X, Hua M, Wang Y, Liu J, Qin Y (2016) High sensitivity NO_2, sensor based on CuO/p-porous silicon heterojunction at room temperature. J Alloy Compd 685:364–369

[6] Selvarajan S, Alluri NR, Chandrasekhar A, Kim S (2016) $BaTiO_3$, nanoparticles as biomaterial film for self-powered glucose sensor application. Sens Actuators B 234:395–403

[7] Komathi S, Muthuchamy N, Lee KP, Gopalan AI (2015) Fabrication of a novel dual mode cholesterol biosensor using titanium dioxide nanowire bridged 3D graphene nanostacks. Biosens Bioelectron 84:64–71

[8] Kumeria T, Maher S, Wang Y, Kaur G, Wang L, Erkelens M, Forward P, Lambert MF, Evdokiou A, Losic D (2016) Naturally derived iron oxide nanowires from bacteria for magnetically triggered drug release and cancer hyperthermia in 2D and 3D culture environments: bacteria biofilm to potent cancer therapeutic. Biomacromol 17:2726–2736

[9] Goto H, Nosaki K, Tomioka K, Hara S, Hiruma K, Motohisa J, Fukui T (2009) Growth of core-shell InP nanowires for photovoltaic application by selective-area metal organic vapor phase epitaxy. Appl Phys Express 2:035004-03500-3

[10] Kasai S, Asai T (2008) Stochastic resonance in schottky wrap gate-controlled GaAs nanowire field-effect transistors and their networks. Appl Phys Express 1:295–302

[11] Koyama T, Hata H, Kim K, Moriyama T, Tanigawa H, Suzuki T, Nakatani Y, Chiba D, Ono T (2013) Current-induced magnetic domain wall motion in a Co/Ni nanowire with structural inversion asymmetry. Appl Phys Express 6:033001–033001–033001–033003

[12] Su D, Ahn H, Wang G (2013) One-dimensional magnetite Fe_3O_4 nanowires as electrode material for Li-ion batteries with improved electrochemical performance. J Power Sources 244:742–746

[13] Wei J, Zhao R, Zhan Y, Meng F, Yang X, Xu M, Liu X (2012) One-step solvothermal syntheses and microwave electromagnetic properties of organic magnetic resin/Fe_3O_4, hybrid nanospheres. Appl Surf Sci 258:6705–6711

[14] Chang M, Wang W, Chung Y (2011) The one-step preparation of nanowires using a facile ultrafiltration technique: the case for biomedical chitosan and/or iron oxide nanowires. J Mater Chem 21:4966–4970

[15] Cao X, Zhang X, Shao H, Feng Y (2014) Fabrication of magnetic Fe_3O_4, nanotubes by electrospinning. Rare Metal Mater Eng 43:2330–2334

[16] Tadić M, Marković D, Spasojević V, Kusigerski V, Remškar M, Pirnat J, Jagličić Z (2007) Synthesis and magnetic properties of concentrated α-Fe_2O_3, nanoparticles in a silica matrix. J Alloy Compd 411:291–296

[17] Yan M, Fresnais J, Sekar S, Berret JF (2010) Growth mechanism of nanostructured super- paramagnetic rods obtained by electrostatic co-assembly. Soft Matter 6:1997–2005

[18] Yan M, Fresnais J, Sekar S, Chapel JP, Berret JF (2011) Magnetic nanowires generated via the waterborne desalting transition pathway. ACS Appl Mater Interfaces 3:1049–1054

[19] Massart R, Dubois E, Cabuil V, Hasmonay E (1995) Preparation and properties of monodisperse magnetic fluids. J Magn Magn Mater 149:1–5

[20] Bee A, Massart R, Neveu S (2015) Synthesis of very fine maghemite particles. J Magn Magn Mater 149:6–9

[21] Berret JF, Sandre O, Mauger A (2007) Size distribution of superparamagnetic particles determined by magnetic sedimentation. Langmuir 23:2993–2999